

OPEN ACCESS

Nano-structures in Al-based alloys

To cite this article: Paola Folegati *et al* 2011 *J. Phys.: Conf. Ser.* **265** 012017

View the [article online](#) for updates and enhancements.

You may also like

- [Enhancement of output performance through post-poling technique on BaTiO₃/PDMS-based triboelectric nanogenerator](#)
Danish Ali, Bin Yu, Xiaochao Duan et al.
- [Preparation of Micro/nano Sized Al₂O₃ Using the By-product of Al-based Composites Hydrolysis Reaction](#)
Xu Guan, Zheng Zhou, Ping Luo et al.
- [Improved Reliability of 278 nm Deep Ultraviolet AlGaIn-Based Flip-Chip Light Emitting Diodes by Using ITO/Al Contact](#)
Woong-Sun Yum, Sang-Youl Lee, Hyun-Soo Lim et al.

ECS
The
Electrochemical
Society
Advancing solid state &
electrochemical science & technology

DISCOVER
how sustainability
intersects with
electrochemistry & solid
state science research

Nano-structures in Al-based alloys

Paola Folegati¹, Martti J Puska² and Torsten E M Staab³

¹ Dipartimento de Fisica e Centro L-NESS, Politecnico di Milano, Via Anzani 42,
I-22100 Como, Italy

² Laboratory of Physics, Helsinki University of Technology, P.O. Box 1100, FI-02015
TKK, Finland

³ Helmholtz Institut für Strahlen- und Kernphysik, Universität Bonn, Nussallee 14-16,
D-53129 Bonn

E-mail: paola.folegati@como.polimi.it

Abstract. The usefulness of first-principles calculations for studying solute-atom clustering in metal alloys is discussed. This usefulness stems directly from the properties predicted by the calculations or via a related interpretation of experimental results. In this paper we review the results of our computational studies on small solute clusters in Al-based alloys. The predicted coincidence Doppler broadening spectra of the positron annihilation method are used to analyse experimental results. The calculated binding energies of small solute atom clusters explain why Cu atoms form two-dimensional platelets on the (100) planes in Al whereas Zn forms three-dimensional clusters.

1. Introduction

First-principles calculations have become an important tool to study various properties of molecules, small aggregates of atoms, and bulk solids. The availability of powerful supercomputers and of several different simulation methods has given an enormous momentum to this subfield in computational physics.

The different simulation approaches can be characterized according to their level of sophistication necessary for describing the structures and phenomena in question. E.g., one can distinguish between nanoscale and subnanoscale descriptions or between static or dynamic descriptions.

In this paper we survey possibilities of interpreting measured positron annihilation data on the basis of computer simulations, showing results for pure metals and for some Al-based alloys. Moreover, we show how first-principles calculations can explain details of solute-atom clustering in these alloys.

2. Why is solute-atom clustering in Al-alloys interesting?

Aluminium alloys are extensively employed in vehicle industry. The process of ageing, discovered by Alfred Wilm [1] already at the beginning of the 20th century, has been recognized as a tool for strengthening these alloys.

Age hardening can be ascribed as precipitation of small particles blocking the crystallographic slip, increasing the resistance to deformation, and hindering the motion of dislocations. It has been recognized that to maximize the hardening one should optimize the size and the distance of the precipitation particles.

Modern experimental techniques have established that the ageing processes in most aluminium alloys are complex and may involve several stages. Typically coherent Guinier-Preston (GP) zones and semicoherent intermediate precipitates may precede the formation of the normally incoherent equilibrium phase. For early decomposition stages, i.e. small agglomerates, the distinction between cluster and GP-zones is still controversially discussed for some alloys.

Atomic clustering, during and immediately after the quenching from the solution-treatment temperature, may also influence the succeeding precipitation process. From this point of view, it is of great interest in the materials science to understand the early stages of clustering.

In order to describe the early stages of clustering only a finite number of host atoms around few solute atoms have to be considered and the modelling can be carried out by means of first-principles electronic-structure calculations, using well-established codes such as VASP and SIESTA [2,3]. In the next section, we will give a brief review of the main computational tools available for the study of clustering and precipitation in alloys.

3. Role of simulations in interpreting measured positron annihilation data (for the solute-atom clustering in metal matrices)

A deeper understanding of the clustering phenomena at the microscopic level is a valuable objective, besides in the area of basic Solid State Physics, also in the field of Materials Science, as it provides guidelines for different thermal and mechanical treatments aimed for improving the materials properties. Clustering and precipitation phenomena in metal alloys are exploited for most applications of these materials. Many desired mechanical and thermal properties of these materials arise from suitable treatments that give rise to precipitation and clustering. Also point defects and impurities play a key role as far as mechanical properties are concerned.

The simulation of clustering and precipitation combines the attention to microscopic aspects (transport and aggregation of atoms in the bulk of a solid matrix) with the interest to industrial applications. The expected results will contribute quantitative data potentially useful for designing compositions and thermal treatments aimed at controlling the size, spatial distribution, and morphology of the aggregates at the nanometer scale. These are all important factors affecting the mechanical and chemical properties of alloys.

At the same time, the comparison of simulations with the existing experimental data gives the possibility to test the accuracy of different schemes and approximations, thus to “sharpen the tool” to be used for computational analyses of atomic rearrangement phenomena. Aluminium alloys are the systems better known from this point of view, and therefore constitute ideal test cases for theories of phase stability. The existence of a rich variety of ordered compounds, solid solutions and metastable phases in aluminium-based systems is an additional point of interest. Understanding phase stability in these systems is a prerequisite for a systematic design and control of alloy properties.

Presently, ab-initio calculations are available on Al-based alloys [4] and some results also on Mg-based alloys [5]. Extensive results are available in particular for:

- vacancy formation energies in bulk metals, both in the local density approximation (LDA) and in the generalized gradient approximation (GGA) of the density functional theory (DFT) and vacancy formation volumes in metals [4,6,7];
- formation enthalpies of ordered compounds in Al-based alloys [4];
- formation energies, enthalpies, and volumes for impurities, vacancy clusters, impurity clusters, and impurity-vacancy complexes in metals [6,10].

However, very few preliminary results are available, for instance, for divacancy formation energies, impurity-divacancy formation energy [5], and, what is most interesting in the present context, for the binding energies of impurity atoms to clusters at different cluster sizes. The last point is a crucial one, if one wants to understand clustering in metal alloys. Ab-initio studies of the energetics should justify the formation and dissolution of clusters, explain the experimental results already obtained from different techniques in Al-based alloys and provide useful input for Kinetic Monte Carlo (KMC) calculations, in which bigger atom systems can be treated (with respect to first-

principle calculations). The existing experimental data on Al-based alloys to be compared with calculated properties range from positron annihilation data to differential scanning calorimetry (DSC), X-ray scattering (XRS), atom probe field-ion microscopy (APFIM), transmission electron microscopy (TEM) and high resolution transition electron microscopy (HRTEM).

The computational tools that have been used until now in this field are:

- Phase-diagram calculation methods (CALPHAD)
- First-principles electronic structure calculations based on DFT
- Kinetic Monte Carlo methods
- Molecular dynamics simulations

A brief description of the main characteristics and limits of each of these methods follows.

3.1. Computational tools

- Methods for calculating phase-diagrams, CALPHAD, use databases of thermodynamic functions to produce accurate phase diagrams and phase equilibria. The advantage of the methods is that they can be applied even to complex multi-component alloys, and for many years they have been used to study many commercial alloys like Al-based, Mg-based and Fe-based alloys. Databases have been generated on the basis of these methods. The limit of this approach is that it cannot predict new thermodynamic data (like existence of new phases) and it is then limited to the analysis of materials for which thermodynamic data are already available.
- First-principles methods have been revealed as a useful complement to CALPHAD approaches by providing energetics and other thermodynamic functions in cases where experimental data are unavailable. An example is the technologically important case of metastable precipitate phases. As far as point defects are concerned, these were studied in the past with empirical models, but recently ab-initio calculations have become the most popular scheme for the calculation of defect formation energies in metals. Although first-principles calculations are slower and far fewer atoms can be handled than in empirical methods, their advantage with respect to empirical methods is their transferability: in multi-component systems, empirical potentials are designed to work in a particular environment, while first-principles calculations are much more flexible: for example, LDA has proved to be a very powerful and sufficiently accurate approach for multicomponent systems in drastically different chemical environments. Although DFT studies are currently limited to a few hundred atoms, many important results about the energetics of defect formation can already be obtained. In addition, first-principles results can generate a large amount of information about the interatomic interaction on a microscopic scale that can be used to fit, or at least put constraints on, simple interatomic potentials. It is difficult, if not impossible, to extract such information from experiments.
- Kinetic Monte Carlo simulations [6] have been revealed to be very well suited for the study of precipitation kinetics in alloys. They allow the treatment of much bigger systems, that is, many more atoms with respect to first-principles calculations. The first simulations were based on a very simple diffusion mechanism: the direct exchange of two nearest-neighbour atoms. Recently, more realistic diffusion mechanisms by vacancy jumps have been introduced in the Monte Carlo method and special attention has been paid to the influence of such diffusion mechanisms on the kinetic pathway during nucleation and growth or phase ordering. Besides the different diffusion mechanisms, these studies have been relying on different models to compute the activation barriers and attempt frequencies of the diffusion events and on different Monte Carlo algorithms. However, in all these studies, the configurational energies and the activation barriers are computed using very simple potentials consisting of short-range pair interactions on a rigid lattice. More accurate potentials exist, but properly accounting the atomic relaxations decreases dramatically the computer efficiency. Monte Carlo studies of precipitation in alloys are based on severe assumptions, when computing both

the configurational energies and the diffusion properties. These assumptions and their consequences on the kinetics of phase transformations have to be questioned and their validity should be tested by comparison with more accurate methods. At the atomic scale, KMC methods are well suited to study diffusion-controlled phenomena, like precipitation kinetics in alloys [7]. These simulations are also useful to test and improve other large scale modelling techniques.

- Another approach to larger systems is molecular dynamics (MD) simulations based on semiempirical models for interatomic interactions. Especially they can be used to study the structures and energetics of solute atom clusters and those of precipitate-host matrix interfaces. An example of the use of MD simulations to the study of clustering in Al-Cu based alloys can be found in ref. [8].

3.2. *What has been done and what has to be done*

It is not a long time since powerful supercomputers have led to the possibility of studying by ab-initio methods many aspects of the energetics and clustering of defects in metal alloys. As far as Al-based alloys are concerned, some work has already been done. Vacancy formation energy in Al has been calculated by many authors, in different schemes of DFT and with different degrees of precision [9]. The later point is related to the supercell size and the related \mathbf{k} -point sampling, to the consideration of relaxations in the lattice and/or in the volume of the supercell itself, and to the type of pseudopotential employed to compute the valence electron wave functions. Results for vacancy formation energies in transition and noble metals, within the LDA, with the order-N Green's function method [11] and for vacancy and substitutional impurities in Al bulk and in different small cluster environments have been computed [10]. Ref. [10] presents also a detailed analysis of the dependence of the calculated quantities on the lattice relaxation, the number of \mathbf{k} -points, and on the supercell size. Other results for vacancy and divacancy formation energies in Al in the LDA and GGA approximations are compared to experimental data in ref. [6] and calculations have been performed also with the KKR Green's function method [9,12]. Impurity diffusion activation energies have also been calculated for Mg, Si, Sc, Zn in Al [14,15]. Recently, a database has been constructed for Al-rich ordered compounds, containing energetics of impurities, formation enthalpies of the ordered compounds, and solubility enthalpies of solute atoms [4]. Ab-initio calculations on vacancy and divacancy formation and binding energies in Al and Mg, together with formation volumes have also been computed [5,6].

First-principles calculations for the energetics of ordered solute - host atom structures or ordered alloys can be used to construct models, such as the mixed-space cluster expansion (MSCE) approach [16], which are applicable to systems of thousands of atoms. MSCE has been used to study, e.g., Cu [17] and Zn [18] clusters in Al alloys. However, at the moment of writing this article, to the best of our knowledge, direct first-principles calculations to study even the smallest solute atom clusters in alloys have not yet been reported in the literature. The reason is the large computer resources they demand.

3.3. *Results on Al and Al-based alloys*

The target of our first-principles calculations of energetics in Al-based alloys is to give an explanation for the observed clustering phenomena in Al-based alloys, both binary (Al-Cu), ternary (Al-Cu-Mg) and, possibly, also quaternary (Al-Cu-Mg-Ag) alloys. Many experimental data are available from Positron Annihilation Spectroscopy (PAS), both lifetime (LS) and coincidence Doppler broadening spectroscopy (CDB), and also from APFIM, TEM, HRTEM and DSC. The existing data seem to give a clear evidence of the tendency of Cu atoms to form platelets along the $\{100\}$ planes in Al [19], while Mg addition indicates that the clusters formed have a more spherical shape. This can be justified on the basis of the calculated binding energies of different atomic species to clusters of different morphology and size. Moreover, the vacancy binding energies to different clusters have to be analysed to deeply understand positron spectroscopy data in these alloys.

4. Why positrons are useful for studying the clustering

The experimental techniques for the analysis of precipitates in alloys can be classified according to “what we want to know”. Table 1 shows the techniques mainly used for different kinds of analysis. Essentially, electron microscopy and TAP (Tomographic Atom Probe) techniques are useful to see precipitates of more than 100-1000 atoms, i.e., clusters of the nanometric size. At the subnanometric level, when there is less than 10 atoms in a cluster, only positron annihilation and XAFS (X-Ray Absorption Fine Structure) can give some information [20,21]. On the other hand at this scale, first-principles calculation can be employed in the simulations. Theoretical approaches for the analysis of bigger (>10 atoms) cluster can only be realized through Kinetic KMC or CALPHAD methods. However, KMC methods need as input data some parameters that have to be computed from first-principles results and others that have to be taken from experimental data.

Table 1. Different method to investigate precipitates in Al-alloys. As a footnote the abbreviations are explained.

Physical information required on precipitates	Experimental technique
Crystal structure	XRD ^a , Electron Diffraction
Internal order	Electron Diffraction, 3D-APFIM ^b , XAFS
Composition	3D-APFIM, CDB-PAS ^c , TEM ^d , XAFS
Spatial distribution	TEM
Nanosize precipitates	TEM, SAXS ^e , SANS ^f , 3D-APFIM
Sub-nanosize precipitates	PAS, XAFS
Volume fraction	TEM, SAXS, SANS, 3D-APFIM
Formation temperature and time	DSC ^g , PALS ^h

^a XRD: X-Ray Diffraction

^b 3D-APFIM: Three-dimensional Atom-Probe Field Ion Microscopy

^c CDB-PAS: Coincidence Doppler Broadening-Positron Annihilation Spectroscopy

^d TEM: Transmission Electron Microscopy

^e SAXS: Small Angle X-Ray Scattering

^f SANS: Small Angle Neutron Scattering

^g DSC: Differential Scanning Calorimetry

^h PALS: Positron Annihilation Lifetime Spectroscopy

The role of positrons in material science has been recognized since long time ago: they are indeed the only non-destructive method that can give information about open-volume defects, and they are sensitive to defect concentrations of the order of 1 ppm. Moreover, since the migration of solute atoms is possible thanks to presence of vacancies, the role of vacancies is a fundamental one. Therefore it is of great importance to have a good probe, like a positron, for the detection of vacancy-like defects. Three kinds of positron traps can be distinguished:

- a) large clusters with high positron affinity,
- b) solute-vacancy clusters,
- c) misfit regions.

The traps of type a) can be found for instance in Fe-Cu alloys (see ref. [22,23]). These are usually big solute clusters (>10 atoms) that tend to trap positrons because the affinity of positrons for the solute is higher than that for the matrix.

Traps of type b) are believed to be the most common in Al-based alloys, where a few atoms usually bind to a vacancy during the migration process. The determination of the percentages of solute and matrix atoms surrounding open-volume defects can be obtained from the analysis of Doppler or Coincidence Doppler Spectra, combined with information from positron lifetime, as will be shown in the next sections [24,25,26].

Traps of type c) form because of the presence of big precipitates, semicoherent or incoherent with the matrix. The presence of these objects causes the formation of a misfit region on the precipitate edge, where open volumes can be formed, and these open volumes act as positron traps.

5. Results from PAS: experimental data and simulations

The interpretation of Doppler spectra of metal alloys requires a careful analysis to extract quantitative information about the chemical environments of annihilation sites. However, this is very difficult to perform only on the basis of experimental data. Therefore, the comparison with simulated curves for which one knows exactly the material composition is a fundamental procedure to support the experimental analysis. Currently, a linear fitting procedure based on the comparison of the alloy spectrum with the spectra for positrons trapped at vacancies in pure constituent metals has been used by the experimentalists in their data analysis [24,27]. The outcome of the fit is the coefficients of the linear combination of the spectra for pure metals. Whereas this procedure tries to attribute the fraction of solute atoms surrounding the vacancy, it cannot account for the effects due to relaxations in- or outwards around the open-volume defects. On the contrary, simulations can account for the different overlaps of the electron and positron densities at the annihilation sites and of the relaxation of atoms around the vacancies. This has revealed to be very important, for instance, in the case of Cu in Al. One of the aims of the simulations is then to verify the adequacy of the fitting procedure used by the experimentalists or to give the recipe for the correct interpretation and for the correction of the linear combination coefficients.

5.1. Electron-positron momentum spectra in Al

The comparison of simulations with experiments can give information also on the size of the open volume defects. Figure 1 (from ref. [28]) shows the results of a study of thermally generated vacancies performed on 5N purity Al single crystals, heated at 417 °C and then quenched in water. Please note that no full trapping of the positrons to vacancies is achieved that way. The momentum density distribution Δ as a function of the momentum p_x is presented in figure 1a without smoothing or symmetrising, in the form of relative difference to a reference spectrum ρ_{bulk} taken for the same single crystals after careful annealing, as given by the equation

$$\Delta = \frac{\rho - \rho_{bulk}}{\rho_{bulk}} . \quad (1)$$

In this presentation, the effect of positron trapping is immediately seen as the deviation of the Δ -curve from the zero line.

Since the annihilation spectrum ρ is related to the trapping fraction F to vacancies, i.e., to the fraction of positrons annihilating at vacancies by

$$\rho = (1 - F)\rho_{bulk} + F\rho_{vac} . \quad (2)$$

Equation (1) can be rewritten as

$$\Delta = F \frac{\rho_{vac} - \rho_{bulk}}{\rho_{bulk}} . \quad (3)$$

This equation tells that the shape of the Δ signal depends only on the morphology of the trap, whereas the intensity is proportional to F . For the experimental details see ref. [28].

The experiment with deformed samples was carried out by using 5N purity polycrystalline Al with compression deformation applied at room temperature up to 50% thickness reduction. The

measurements were performed at liquid nitrogen temperature with the same procedure as used for the quenched specimens. The results are shown in figure 1b, once more in terms of the relative difference to bulk data (equation (1)).

The comparison of figures 1a and 1b shows the following features of similarity in the Δ curves: a) a broad maximum centered at $p_x=0$; b) a well-defined peak near $p_x=8\times 10^{-3} m_0c$; c) a negative tail in the high momentum region. The same features can be found in previous CDB measurements for defected Al [29,30]. On the other hand, it may be noted that the curves in figures 1a and 1b cannot be scaled to a common master curve, as it would be predicted by equation (3) if the morphology of the traps were the same in quenched and in deformed Al.

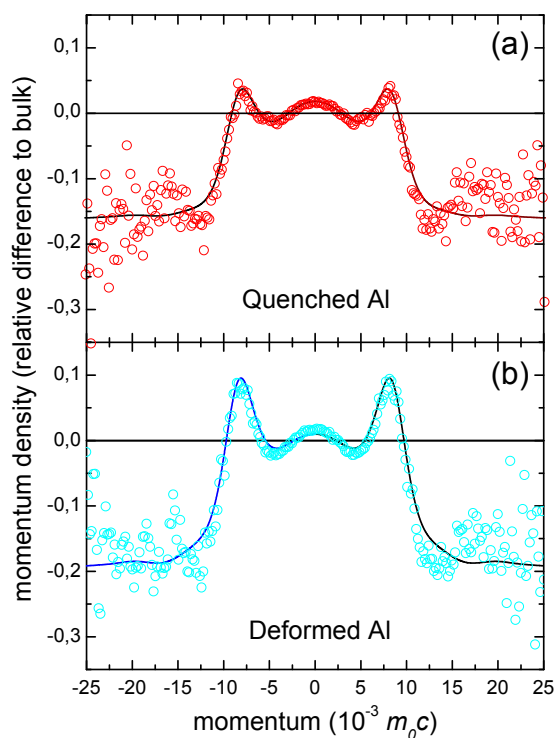


Figure 1. CDB spectrum for defected Al (relative difference to annealed Al). The solid line is the result of an ab-initio LDA calculation (see text).

Ab-initio calculations for the e^+e^- momentum densities were performed for bulk Al and for various geometries of open-volume positron traps, with the aim of testing the possibility to reproduce the similarities and the differences in the curves in figures 1a and 1b, and to isolate the physical mechanisms to which they are to be ascribed.

A general introduction to ab-initio calculations of positron annihilation characteristics in solids can be found in ref. [31]. The procedure adopted for the simulation of curves in figures 1a and 1b was as follows. Valence electron densities were computed self-consistently in the LDA framework. The computation was carried out by employing the VASP code [35] with the projector augmented-wave (PAW) method [34] to account for the electron – ion core interaction. The PAW method enables plane-wave expansions for pseudo valence wavefunctions used in self-consistent calculations and the post-construction of all-electron valence wavefunctions resulting in accurate electron momentum densities [32]. In the calculations the Brillouin zone was sampled using a $3\times 3\times 3$ Monkhorst-Pack \mathbf{k} -point mesh [33]. A cutoff of 241 eV was used when calculating the pseudo valence wavefunctions and a cutoff equivalent to $70\times 10^{-3} m_0c$ was used when forming all-electron valence wavefunctions.

Using the total charge density from the VASP-PAW calculations and the LDA [36] for electron-positron correlation potential, positron states were calculated on a three-dimensional real-space point grid [37]. The so-called “conventional scheme”, in which the localized positron density does not affect the electron density, was used to describe trapped positrons. The annihilation rates of self-consistent all-electron valence states and atomic core electron states were calculated within the LDA [38] for the electron-positron correlation. These partial annihilation rates were used as weighting factors when calculating momentum densities of annihilating electron-positron pairs within the so-called state-dependent enhancement scheme [39,41].

The momentum distributions corresponding to valence electrons were obtained by the three-dimensional Fourier transform on a cubic grid with the spacing of $0.67 \times 10^{-3} m_0c$ and those for the core electrons on a dense radial grid using parameterized forms of the positron wavefunction [40].

A cubic supercell of 108 atomic sites in a periodic superlattice was used for the simulation of bulk and of defected Al. Vacancy-like defects were simulated by empty atomic sites. The nearest neighbours of the missing atoms were moved isotropically from their normal lattice sites in order to reproduce the local relaxation in the proximity of the empty site. The explored range of possible relaxations was from 2% outward to 6% inward. Larger inward displacements are expected for positron traps associated to dislocations, which can be essentially described as distorted vacancies with a reduced free volume [41]. One-dimensional momentum distributions were computed for bulk and for defected Al and convoluted with a Gaussian (FWHM= $3.5 \times 10^{-3} m_0c$) to simulate the experimental resolution. Then they were used to calculate the relative difference Δ by equation (2) (with $F=1$).

The Δ curves in figure 2 correspond to different values of the linear relaxation at the empty site. The theoretical curves for the 0 and 4% inward linear relaxation curves are also reported in figure 1 after vertical scaling to account for a trapping fraction $F < 1$. The best fit is for $F=0.34$ for the quenched sample and $F=0.64$ for the deformed sample.

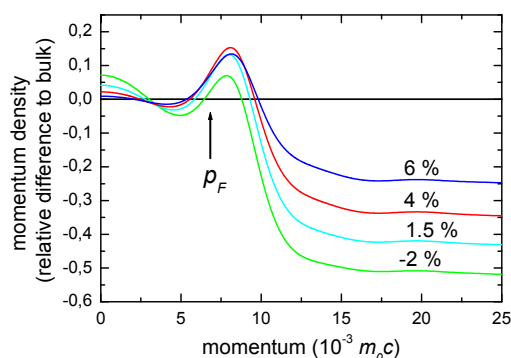


Figure 2. Calculated Δ -curves for positron trapping at an Al vacancy. Labels on the curves show the isotropic inward relaxation of the nearest-neighbour positions (here, and in the following figures, negative values are conventionally attributed to outward relaxations). The Fermi momentum p_F is denoted by the upward arrow.

The simulation offers the possibility to isolate the different factors that contribute to the formation of the characteristic shapes of the Δ curves. The following considerations can be made.

- The broad maximum at $p_x=0$ comes from the narrowing of the valence electron momentum distribution associated with the reduction of electron density at the defect. This effect is well known since the early studies of positron trapping at defects in metals [44], but is clearly visible also in semiconductors [29,30,42,43].
- The negative value taken by Δ at high momentum is simply due to the reduction of the core electron contribution to annihilation, which always occurs when the positron wavefunction becomes localized in an open-volume defect.
- The peak seen in figures 1 and 2 near to $8 \times 10^{-3} m_0c$, i.e., just beyond the Fermi cutoff of the valence electron distribution, is due to the quantum confinement of the positron wavefunction in a region of atomic dimensions. The motion of the confined particle implies a non-negligible contribution to the total momentum carried away by the annihilation radiation. Figure 3 shows

computed momentum distributions for positrons trapped at vacancy-like defects with different degrees of relaxation. A visual gauge of the momentum scale of figure 5 is provided by the horizontal double-head arrow, which shows the minimum momentum indetermination that, by the uncertainty principle, corresponds to the quantum confinement over a distance equal to the Al lattice constant of 4.0 Å.

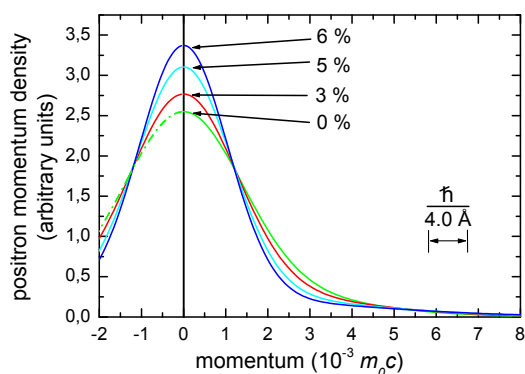


Figure 3. Positron momentum distributions for positrons trapped in vacancy-like defects. The labels on the curves indicate the inward displacement of the nearest neighbours of the empty atomic site. The horizontal bar shows the expected momentum width for quantum confinement within a box with a dimension of 4.0 Å.

The most relevant effect of positron motion is to smear the Fermi cutoff. Since the smearing enhances the counting rate beyond the Fermi cutoff, additional counts fall in a region where the counting rate in the bulk metal reference spectrum is low, thus producing a peak in the ratio curves used for presenting the CDB data. The momentum contribution of a confined positron can be added to the electron momentum distribution without including any other effect of trapping (namely, reduction of the density of valence electrons at the vacancy and changes in the annihilation rates with different electron states). This is done by convoluting the momentum distribution calculated for bulk Al, where there is no effect of positron confinement, with the positron momentum distribution that is expected in the case of trapping at a vacancy-like defect (as depicted in figure 3). In any real experiment, the visibility of the effect would depend on the resolution of the apparatus, which determines the sharpness of the Fermi cut-off.

In summary, the CDB technique shows a sensitivity to the local geometry, since the distributions taken for positrons trapped at quenched-in thermal vacancies or at dislocation-associated vacancy-like defects are clearly distinguishable.

5.2. Electron-positron momentum spectra in Al-based alloys

In the case of alloys, when CDB measurements are applied to the study of precipitations (for a review, see ref. [45]), the confinement peak can be a disturbance, as it is partially superimposed to the additional structures that are due to the decoration of vacancy-like defects by minority alloy components. This makes it impossible to reproduce the CDB distribution for an alloy as a linear combination of the distributions measured for annealed samples of pure elements. An empirical attempt to circumvent the problem has been proposed by Somoza et al. [27], who have obtained good fits of their experimental data for Al-Cu-based alloys by using linear combinations of distributions measured for defected samples of the alloy components.

First-principles calculations have been performed also for Al-based alloys, to study the possibility of quantitative chemical analysis of vacancy-solute complexes [28,29]. Figure 4 shows a comparison of simulated curves with CDB data for an Al-Cu alloy, as-quenched (a) and after 1 min ageing at 150°C (b), in order to find the most probable complexes present in the samples. The details of the procedure are explained in ref. [28].

The annihilation spectrum can be given in this case by equation (2) modified to account for the different types of traps (index k):

$$\rho = (1 - F)\rho_{bulk} + F \sum_k C_k \rho_{vac,k} \quad (2')$$

The fitting procedure by Somoza et al. [27] uses this form with $\rho_{vac,k}$'s obtained by measuring the spectra for elemental deformed metals.

In the case of the as-quenched sample the procedure by Somoza et al. gives 23 ± 1.5 % as the average number of solute atoms surrounding the vacancy, i.e., roughly three Cu atoms among the 12 nearest neighbours of the vacancy. This is in agreement with the analysis based on the first-principles calculations and shown in Fig. 4a. The figure shows best one-component fits (the trapping fraction is fitted) obtained with spectra calculated for vacancy-Cu defects with two, three and four Cu atoms as the dash-dotted (blue), solid (red) and dotted (black) lines, respectively.

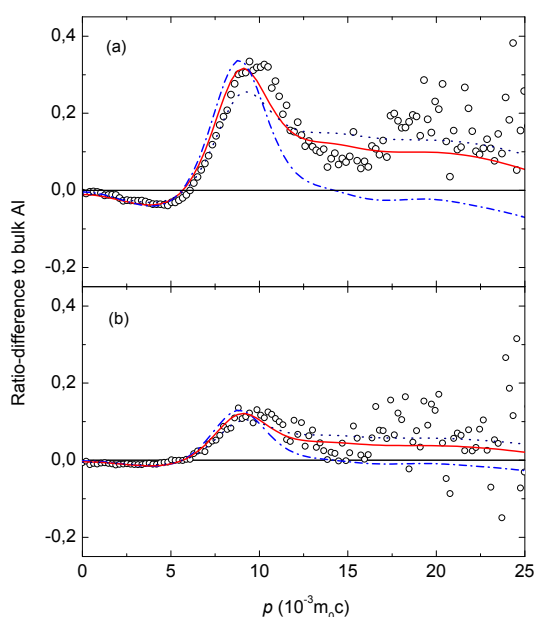


Figure 4. Comparison of simulated curves with CDB data for an Al-Cu alloy, as-quenched (a) and after 1 min ageing at 150°C (b). Dash-dotted (blue), solid (red) and dotted (black) lines show the best one-component fits obtained for vacancy-Cu defects with two, three and four Cu atoms, respectively.

In the case of the aged sample in Fig. 4b, we get a reasonable fit with three or four Cu atoms, resulting in trapping fractions of 24 and 17%, respectively. In this case the procedure by Somoza et al. gives 33 ± 5 % for the Cu contribution, that is, about four Cu atoms, and a trapping fraction of 18 ± 1 % is found.

In the case of ternary (AlCuMg) and quaternary (AlCuMgAg) alloys, the first-principles simulations of CDB spectra show that the procedure by Somoza et al. can give good estimates for the Cu and Ag concentrations and for the sum the Al and Mg concentrations but not for the Al and Mg concentrations separately. However, the conclusion about determining the Mg concentration is unclear because the calculated and measured CDB spectra for Mg are clearly different.

5.3. What is the degree of precision of the calculations

When studying defects in solids by positrons we observe changes in annihilation characteristics relative to well-known systems, typically perfect bulk lattices of elemental solids or monovacancies in them. Experimentally, the former are obtained by a careful annealing treatment and the latter can be prepared in a controlled manner by electron irradiation of the perfect bulk samples. The conclusions drawn from the changes about the defect structures and their development are then on a firm basis. This philosophy is applied further when analysing the positron data with the help of theoretical predictions. Calculated absolute values, for example the momentum distributions of annihilating

electron-positron pairs, depend strongly on the treatment of the many-body effects between electrons and between electrons and the positron even for delocalized positron states in perfect lattices (For a recent work, see ref. [49]). DFT within the LDA or GGA is at the moment the only practical and reliable enough method to simulate defects in solids. However, as a mean-field theory DFT cannot accurately describe the electron-electron or electron-positron correlation effects. But when taking differences between different systems errors cancel. For example, the predicted ratio-difference curves between transition metals and Al show a good agreement with experiment [37].

Typically, the LDA underestimates slightly, usually by about 1 – 2 % the lattice constants and there may be small uncertainties in the ionic structures of the defects. The predicted positron annihilation characteristics are very sensitive to the atomic positions. In theory-experiment comparisons one approach is therefore to adjust slightly the lattice constant or in the case of vacancies in elemental solids the symmetric relaxation of atoms neighbouring the vacancy.

For example, the results for the Al-Cu alloy discussed above are obtained by adjusting the Al lattice constant to reproduce the experimental lifetime for trapped positrons in the alloy. In this case, the lifetime is about 20 ps shorter than that for Al indicating a strained lattice around the defect. The reduction of the Al lattice constant by 4 % reproduces the decrease of the lifetime. The substitution of the host atoms by solute atoms around a vacancy causes changes in the annihilation characteristics which depend on the solute atom in question. The changes are due to the changes in the electronic structure and depend also on the specific relaxation of the solute atom. In the case of Cu the changes are relatively large and therefore one can conclude that the analysis of the experimental data by the simulation results can distinguish the number solute atoms around the vacancy with the accuracy of about one atom. This is certainly enough in order to draw conclusions about the details of the clustering process.

6. Preliminary first-principles results for clustering in Al-based alloys

First-principles calculations have been performed for Al-based alloys [46] to understand, on the basis of energetics, the early stages of solute-atom clustering. Calculations of vacancy and divacancy formation energies and the impurity solubility enthalpies have also been performed in different schemes. Comparisons with existing literature values show that for these energies accurate results converged with respect to the different computation parameters can be achieved.

All the calculations of the formation and binding energies are carried out with the VASP code. It allows a comparison between LDA and GGA, and precision tests as a function of the supercell size and the number of \mathbf{k} -points. Moreover, it allows the relaxation of both the atomic positions and the configurations are shown. The two-dimensional clusters are compact configurations on the (100) plane.

Although our main goal is to study the early stages of precipitation in Al-Cu-Mg(-Ag) alloys we have already performed calculations, in addition to Cu clusters in Al, also for Zn clusters in Al. This is because small Cu and Zn precipitates behave remarkably differently in Al and we want to put our first-principles approach in a stringent test. Specifically, small Cu clusters are two-dimensional platelets on (100) planes whereas small Zn clusters are three-dimensional (see, e.g., refs. [17,18,48] and the references therein).

Figures 5 and 6 show the binding energy per cluster atom for Zn and Cu clusters in Al, respectively. The clusters are built up by filling adjacent lattice sites. The two-dimensional clusters form platelets on the (100) plane. The increase of the average binding energy as the size of the cluster increases reflects the stability of the crystal growth.

The favoured configurations are two- and three-dimensional for Cu for Zn clusters, respectively. This result, which is in agreement with experimental APFIM [19,47] and HRTEM [19] data, can be interpreted on the basis of the following argument. The Wigner-Seitz radius of Zn is very close to that of Al, and therefore the elastic stress created in the matrix is minimized by the three-dimensional configuration. The Wigner-Seitz radius of Cu is smaller than that of Al. Therefore, Cu tends to create a quite a huge stress in the matrix that is minimized if the clusters form on the (100) plane of Al and the

relaxation of Al atoms takes place essentially only along the [100] direction perpendicular to that plane. This is the soft direction in the fcc-Al for atomic displacements, and according to our calculations the relaxation of Al atoms below and above the (100) Cu platelet is substantial towards the platelet.

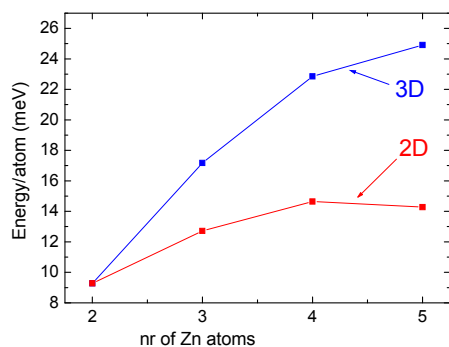


Figure 5. Binding energy per Zn atom in Zn clusters in Al. Results for two- and three-dimensional configurations are shown. The two-dimensional clusters are compact configurations on the (100) plane.

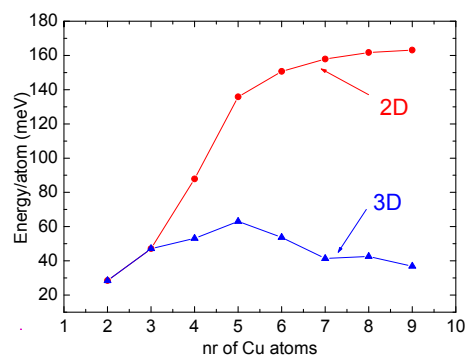


Figure 6. Binding energy per Cu atom in Cu clusters in Al.

7. Summary

In this paper we have first reviewed methods to simulate the properties of metallic alloys and the results obtained especially by the first-principles electronic structure calculations. We have advocated also another route of using the ab-initio results. Namely, in the case of positron annihilation methods we discussed how the theoretical predictions can be used to support the interpretation of measured data. The analysis of the formation of vacancy-solute-atom complexes in Al-Cu alloys was used as an example. Finally, we have presented preliminary results for the energetics of Cu and Zn clusters in Al. They give microscopic information about the early stages of the precipitation process and they can be used as the starting point for Monte-Carlo simulations for the precipitation kinetics.

References

- [1] Wilm Alfred 1911 *Metallurgie* **8** 255 (1911)
- [2] <http://cms.mpi.univie.ac.at/vasp/>, Sun G, Kürti Rajczy J P, Kertesz M, Hafner J and Kresse G 2003 THEOCHEM - *J. Molec. Struct.* **624** 37
- [3] Soler J M, Artacho E, Gale J D, Garcia A, Junquera J, Ordejón P and Sánchez-Portal D 2002 *J. Phys. Cond. Matter* **14** 2745
- [4] Wolverton C and Ozoliņš V 2006 *Phys. Rev. B* **73** 144104
- [5] Uesugi T, Kohyama M and Higashi K 2003 *Phys. Rev. B* **68** 184103
- [6] Carling K, Wahnström G, Mattson T, Mattson A, Sandberg N and Grimvall G 2000 *Phys. Rev. Lett.* **85** 3862
- [7] Martin G and Soisson F 2006 *Adv. Eng. Mater.* **8** 1210
- [8] Hu S Y, Baskes M I, Stan M and Chen L Q 2006 *Acta Mater.* **54** 4699
- [9] Hoshino T, Papanikolaou N, Zeller R, Dederichs P H and Asato M 1999 *Comp. Mater. Sci.* **14** 56
- [10] Turner D E, Zhu Z Z, Chan C T and Ho K M 1997 *Phys. Rev. B* **55** 13842
- [11] Korzhavyi P A, Abrikosov I A, Ruban A V and Skriver H L 1999 *Phys. Rev. B* **59** 11693
- [12] Hoshino T, Asato M, Zeller R and Dederichs P H 2004 *Phys. Rev. B* **70** 094118
- [13] Clouet E, Nastar M and Sigli C 2004 *Phys. Rev. B* **69** 064109
- [14] Sandberg N and Holmestad R 2006 *Phys. Rev. B* **73** 014108

- [15] Turchi P E A, Drchal V, Colinet C, Kaufman L and Liu Z K 2005 *Phys. Rev. B* **71** 094206
- [16] Lax D B, Ferreira L G, Froyen S and Zunger A 1992 *Phys. Rev. B* **46** 075111
- [17] Wang J, Wolverton C, Müller S, Liu Z-K and Chen L-Q 2005 *Acta Mater.* **53** 2759
- [18] Müller S, Wolverton C, Wang L-W and Zunger A 2001 *Europhys. Lett.* **55** 33
- [19] Ringer S P and Hono K 2000 *Materials Characterization* **44** 101
- [20] Staab T E M, Zamponi Z, Haaks M, Modrow H and Maier K 2007 *Phys. Stat. Sol. (rrl)* **1** 172
- [21] Klobes B, Staab T E M and Dudzik E 2008 *phys. stat. sol. (rrl)* **3** doi: 10.1002/pssr.200802067
- [22] Nagai Y, Takadate K, Tang Z, Ohkubo H, Sunaga H, Takizawa H and Hasegawa M 2003 *Phys. Rev. B* **67** 224202
- [23] Eldrup M, Singh B N, Edwards D J, Nagai Y, Ohkubo H and Hasegawa M 2004 *Mater. Sci. Forum* **445-446** 21
- [24] Somoza A, Petkov M P, Lynn K G and Dupasquier A 2002 *Phys. Rev. B* **65** 094107
- [25] Folegati P, Makkonen I, Ferragut R and Puska M J 2007 *Phys. Rev. B* **75** 054201
- [26] Folegati P, Dupasquier A, Ferragut R, Iglesias M M, Makkonen I and Puska M J 2007 *phys. stat. sol. (c)* 3493
- [27] Somoza A, Dupasquier A, Polmear I J, Folegati P and Ferragut R 2000 *Phys. Rev. B* **61** 014454
- [28] Calloni A, Dupasquier A, Ferragut R, Folegati P, Iglesias M, Makkonen I and Puska M J 2005 *Phys. Rev. B* **72** 054112
- [29] Ambigapathy R, Corbel C, Hautojärvi P, Manuel A A and Saarinen K 1995 *J. Phys.: Condens. Matter* **7** L683
- [30] Ambigapathy R, Corbel C, Hautojärvi P, Manuel A A and Saarinen K 1996 *Appl. Phys. A* **62** 529
- [31] Puska M J and Nieminen R N 1994 *Rev. Mod. Phys.* **66** 841
- [32] Makkonen I, Hakala M and Puska M J 2008 *J. Phys. Chem Phys.* **128** 244101
- [33] Monkhorst H J and Pack J D 1976 *Phys. Rev. B* **23** 5048
- [34] Blöchl P E 1994 *Phys. Rev. B* **50** 17953
- [35] Kresse G and Joubert D 1999 *Phys. Rev. B* **59** 1758
- [36] Boronski E and Nieminen R M 1986 *Phys. Rev. B* **34** 3820
- [37] Makkonen I, Hakala M and Puska M J 2006 *Phys. Rev. B* **73** 035103
- [38] Alatalo M, Barbiellini B, Hakala M, Kauppinen H, Puska M J, Saarinen K, Hautojärvi P and Nieminen R M 1996 *Phys. Rev. B* **54** 2397
- [39] Barbiellini B, Hakala M, Puska M J, Nieminen R M and Manuel A A 1997 *Phys. Rev. B* **56** 136
- [40] Alatalo M, Kauppinen H, Saarinen K, Puska M J, Mäkinen J, Hautojärvi P and Nieminen R M 1995 *Phys. Rev. B* **51** 4176
- [41] Häkkinen H, Mäkinen S and Manninen M 1990 *Phys. Rev. B* **41** 12441
- [42] Ambigapathy R, Manuel A A, Hautojärvi P, Saarinen K and Corbel C 1994 *Phys. Rev. B* **50** 2188
- [43] Hasegawa M, Tang Z, Chiba T, Saito M, Kawasuso A, Akahane T, Li Z Q, Kawazoe Y and Yamaguchi S 1997 *Mater. Sci. Forum* **255** 414
- [44] Marceau R K W, Ferragut R, Dupasquier A, Iglesias M M and Ringer S P 2006 *Mater. Sci. Forum* **519-521** 197
- [45] Dupasquier A, Kögel G and Somoza A 2004 *Acta Mater.* **52** 4707
- [46] Folegati P, Kohlbach I, Makkonen I, Puska M J and Staab T E M 2008 to be published
- [47] Hono K 1999 *Acta Mater.* **47** 3127
- [48] Müller S, Wang L W, Zunger A and Wolverton C 1999 *Phys. Rev. B* **60** 16448
- [49] Sormann H and Kontrym-Sznajd G 2006, *Phys. Rev. B* **73** 075111